JOURNAL OF Materials Chemistry Communication

Particle morphology and microstructure in the mesoporous silicate SBA-2

Hazel M. A. Hunter,[a] Alfonso E. Garcia-Bennett,[a] Ian J. Shannon,[b] Wuzong Zhou[a] and Paul A. Wright*[a]

[a]*School of Chemistry, University of St Andrews, Purdie Building, North Haugh, St Andrews, Fife, UK KY16 9ST. E-mail: paw2@st-andrews.ac.uk*
[b]*School of Chemical Sciences, The University of Birmingham, Edgbaston, Birmingham, UK B15 2TT*

Received 11th September 2001, Accepted 9th November 2001
First published as an Advance Article on the web 26th November 2001

The mesoporous solid SBA-2, prepared at room temperature in alkaline pH using the gemini surfactant $[CH_3(CH_2)_{15}N(CH_3)_2(CH_2)_3N(CH_3)_3]^{2+}$ can adopt hollow sphere (*ca.* 100 μm diameter), flat plate (50 μm across) and small sphere (1–2 μm diameter) morphologies. Plates appear to be formed directly by fracturing of the hollow spheres. The nanostructure of these materials is consistent with templating around close packed micelles. X-Ray diffraction and high resolution imaging show that the structure of these preparations ranges from mainly hexagonal to mainly cubic close packing.

Ordered mesoporous silicas, prepared by templating with surfactants,[1–3] offer great promise as catalyst supports[4,5] and as molecular sieves for the separation of molecules that are too large to fit in the pores of crystalline zeolites.[6,7] Silicas that display two-dimensional long range order, such as MCM-41[1] and SBA-15[8] (space group *p6mm*), have been studied in the most detail, but a number of silicas that display long range order in three dimensions have also been discovered. Of these, the detailed structures of MCM-48[9] ($Ia\bar{3}d$), SBA-1[10] and SBA-6[11] (both $Pm\bar{3}n$), SBA-16[11] and SBA-2[12] have been elucidated by high resolution electron microscopy (HRTEM) and electron diffraction,[13] although previous work on SBA-2 by ourselves[12] and others has been limited by inherent stacking disorders. Current models for the structure of as-prepared SBA-2 are based on silicate condensed between a close packed array of spherical micelles, such that removal of the template by calcination gives interconnected cages. Although the original work of Stucky and coworkers[2,3] indicated that the cages in their samples were arranged in a hexagonal close packed array, HRTEM of our own materials revealed the presence of stacking faults and regions of the cubic close packed or face centred cubic polytype.

We consider here the particle morphology of SBA-2 and then go on to investigate how this is related to its microstructure. As well as giving information on the way in which these solids form, the particle morphology is likely to influence the performance of these materials[14] in potential applications. For example, hollow spheres[15] are desired as controlled release capsules for drugs and other chemicals. Oriented porous films,[16] meanwhile, are of interest in membrane applications. Whereas other three-dimensional mesoporous solids such as MCM-48[9] and SBA-1[10] can be prepared with crystal-like morphologies, we have not observed such features with our SBA-2 preparations.[17] Instead we have seen small solid spheres, flat sheet particles with complex and irregular domain structures, and larger spherical hollow forms.

SBA-2 was synthesised from a homogenised mixture with molar composition: 0.025–0.05 surfactant : 0.5 tetramethylammonium hydroxide (TMAOH) : 1 tetraethylorthosilicate (TEOS) : 45–150 H_2O. The gemini surfactant, $CH_3(CH_2)_{15}N(CH_3)_2(CH_2)_3N(CH_3)_3Br_2$,[18] was added to the aqueous solution of TMAOH, followed by addition of the TEOS. SBA-2 precipitated from the mixture over a reaction period of two hours at room temperature, which was either stirred (at rates of 300 or 500 rpm) or left static. The mesoporous solid was recovered by filtration, washed repeatedly with distilled water and dried overnight in air at room temperature. Calcination at 550 °C (1 h N_2, 6 h O_2) removed the surfactant to give the porous silicate.

Powder X-ray diffraction patterns were collected at ambient temperature using Cu-Kα radiation, $\lambda = 1.5418$ Å, on a Philips PW 1830 diffractometer equipped with a secondary monochromator. Scanning electron microscopy (SEM) images were obtained from a JEOL JSM-5600 scanning electron microscope operating at a voltage up to 30 kV and with an optimal resolution of 3 nm. HRTEM images were recorded using a JEOL JEM-200CX electron microscope, operating at 200 kV. SBA-2 samples were prepared by adhering them onto a holey carbon film, supported on a Cu grid, before transferring them into the specimen chamber. The objective lens parameters, $C_S = 0.41$ nm and $C_C = 0.95$ nm gave an interpretable point resolution of *ca.* 1.85 Å. Images were recorded along high symmetry zone axes at magnifications of 24000× to 49000×. It was found that the as-prepared samples decomposed in the electron beam, thus all HRTEM investigations are based on calcined samples. In general, and unless stated otherwise, the fine powders were *not* ground prior to depositing them onto the TEM specimen grid.

The powder X-ray diffraction profiles of the samples are characteristic of SBA-2,[2,3] and may be indexed on a hexagonal unit cell, typically for as-prepared samples under these conditions $a = 56(1)$ Å, $c = 92(2)$ Å, whereas for the calcined samples $a = 48(1)$ Å, $c = 80(2)$ Å. Some variation in the peak intensities is observed (Fig. 1), particularly in those reflections which are expected from the hexagonal close packed (hcp) array but not for the cubic close packed (ccp) stacking variant, for which the equivalent cubic cell parameter would be *ca.* 69 Å. For example, reflection $(103)_{hex}$ is weak or absent in some patterns, indicating a larger proportion of the cubic stacking sequence and/or stacking faults.

Scanning electron microscopy and low resolution transmission electron microscopy of SBA-2 samples indicates the presence of large hollow spheres, flat sheets and much smaller spherical particles (Fig. 2(a)–(c)). SEM images of the hollow spheres show that they range from 100–180 μm in diameter and the outer wall is typically *ca.* 2 μm thick. Similar particles were

 DOI: 10.1039/b108259k

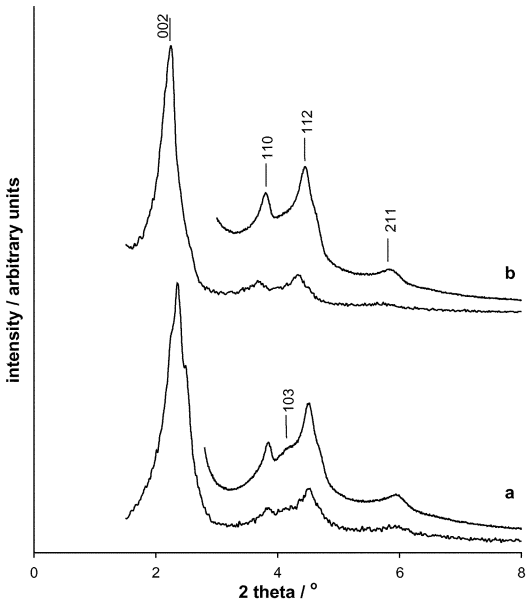

Fig. 1 Powder X-ray diffraction patterns of two calcined SBA-2 samples showing the variation in the intensities of the reflections. For each solid patterns were collected for 10 minutes between 2θ 1.5–8° and overnight (>12 h) between 2θ 3–8°. The reflections are indexed in the hexagonal system only. The reflection $(103)_{hex}$ indicated for sample (a) is only expected in the hexagonal close packed array, and not in the cubic close packed variant.

observed close to the liquid surface during the SBA-2 synthesis according to optical microscopy. This mid-synthesis observation suggests that they may arise from silicate condensation around air bubbles. The flat sheet particles (up to 50 μm in extent) are uniformly thin and possess sharp edges (Fig. 2(c)), suggesting that at one time they were part of a much larger body. A similar range of silicate morphologies have been observed[19] in biphasic emulsion systems as a function of stirring speed. The hollow spheres and flat sheets make up around 20% of the samples, with the remainder being composed of the much smaller spheres. The amount of hollow spheres appears to decrease with increased stirring rate.

The much smaller, solid, spherical particles have diameters of a few μm and are similar in shape to those of MCM-41 described previously.[20] Unlike other well defined mesoporous structures (*e.g.* MCM-48 and SBA-1) no crystal-like forms were observed. Indeed, low resolution transmission electron microscopy reveals that the particles contain smooth, curved surfaces (Fig. 3(a)). Typically these particles have dimensions in the region 1–2 μm and possess regular mesoporous order throughout. High resolution transmission electron microscopy (HRTEM) of these small spherical particles (Figs. 3(b) and (c)), limited to thin edge locations, reveals a complex domain structure. For the purposes of this discussion a domain is defined as an ordered region possessing a single characteristic orientation of planes containing close packed pores. Perpendicular to this plane, the domains possess stacking faults of variable frequency. Two regions are examined in detail. Fig. 3(b) (from which Fig. 2 of reference 12 was taken) shows at least three domains, within which regions possessing both hcp and ccp regions are observed, with a predominance of ccp stacking. At the domain boundaries it appears that a cage may be surrounded (in the plane of projection) by five or seven other cages, compared to the six expected within a domain. Micelle packing arrangements must adapt to enable formation of these sequences. A second region of a small solid particle is illustrated in Fig. 3(c). The large domain (characterised by a single orientation of a close packed plane) is observed to contain more than ten stacking faults. Away from these stacking faults the domain is of the cubic close packed polytype. On the basis

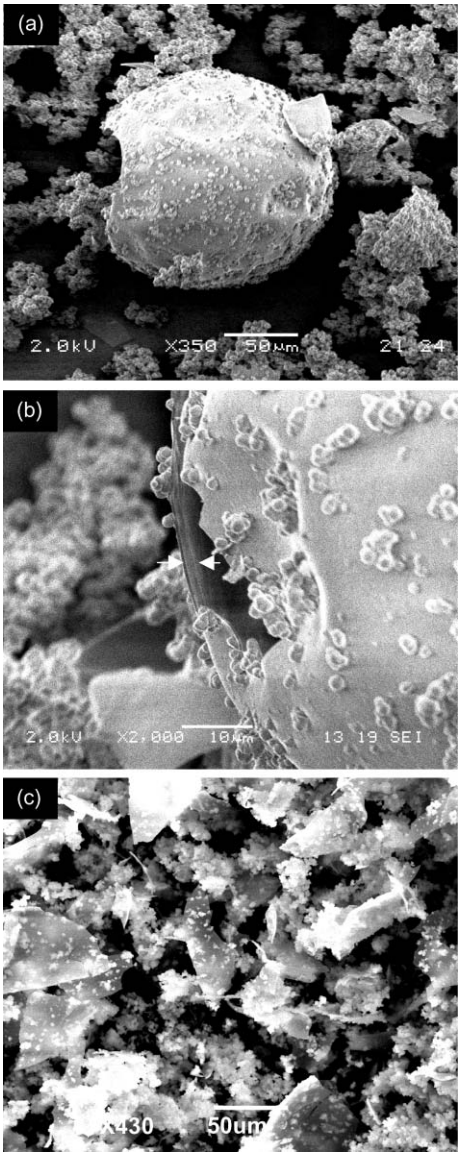

Fig. 2 Scanning electron micrographs of SBA-2. A micrograph (a) from a synthesis, initial composition: 0.05 surfactant : 0.5 TMAOH : TEOS1 : 50 H_2O, stirring rate *ca.* 300 rpm) shows hollow spheres and small solid particles. A close-up of a hole in one of the larger spheres shows the shell to be around 2 μm thick (b). A micrograph of a second preparation (composition 0.027 surfactant : 0.5 TMAOH : TEOS : 45 H_2O, stirring rate *ca.* 500 rpm) shows a predominance of irregular flat-sheet fragments, 50 μm or more across, and small spherical particles.

of XRD and HRTEM it appears that under certain conditions the dominant phase in the SBA-2 family can be the cubic polytype.

HRTEM of the particles that have a plate-like or flat-sheet morphology are shown in Fig. 4(a). Similarly to the spherical particle, the sheets are made up of a large number of irregularly arranged SBA-2 type domains, the dimensions of which may extend to the μm range. Determination of the view direction from electron diffraction is hampered by the intergrowth system within each particle. To confirm that the larger, hollow spheres were also made up of SBA-2 mesoporous silica, intact hollow spheres were isolated from the matrix, crushed and examined by HRTEM. As well as typical structures that are predominantly cubic close packed with frequent twin planes, images down [100] of the face centred cubic cell were also observed, confirming the structure (Fig. 4(b)).

In summary, the SBA-2 family of mesoporous silicates, which are thought to condense around close packed arrays of spherical micelles, show three particle morphologies: small

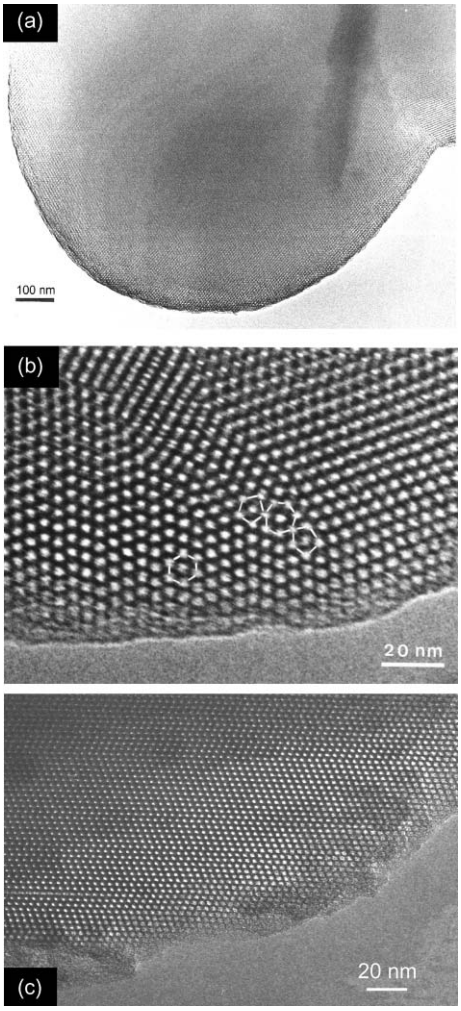

Fig. 3 Transmission electron micrographs of small spherical particles: (a) shows a single rounded particle, (b) is an underfocus high resolution micrograph of a region showing stacking faults within domains and defects at the domain boundary (5-, 6- and 7-member nearest neighbour 'rings' are highlighted) and (c) is of a particle with a single orientation of one set of close packed planes, but with stacking faults in an otherwise cubic array.

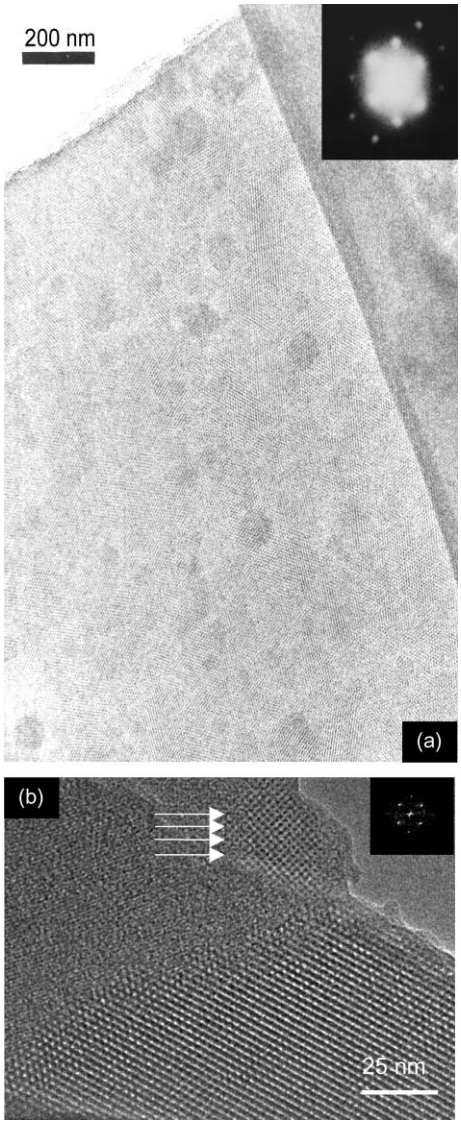

Fig. 4 TEM images of SBA-2 showing: (a) a flat sheet, with associated selected area diffraction pattern, (b) a crushed hollow sphere, displaying a typical arrangement of pores. The arrows in (b) highlight a lattice image down [100] of the cubic unit cell, together with a computer simulated diffraction pattern from this selected area.

solid spheres, plates, and larger hollow spheres. One explanation for the hollow sphere morphology is a mechanism by which the composite organic/silicate solid is formed around air bubbles. The sheet-like particles may arise directly at solvent/air interfaces or from collapse of the hollow spheres whereas the small spherical particles are believed to form in the bulk suspension. The decreased amount of hollow spheres at high stirring speeds suggests that they can be fractured with increased agitation, giving rise to the plates that are observed. HRTEM reveals a high degree of disorder in SBA-2 that accounts for the lack of crystal-like particle morphologies that are seen in other 3D ordered solids. This disorder results from both the irregular arrangement of domains (within spheres and sheets) and also stacking disorder within the domains. Evidence is presented that in certain preparations the dominant phase is the cubic stacking variant (referred to previously[12] as STAC-1). This is supported by X-ray powder diffraction patterns that do not show distinct maxima characteristic of the hexagonal phase. These structural features are similar to those reported recently[21] for the mesoporous solid SBA-12, prepared under acid conditions in the presence of the $C_{18}EO_{10}$ surfactant copolymer. The SBA-12 large pore silica structure also consists mainly of face centred cubic arrays.

This work was supported by EPSRC studentships to H. M. A. H, and A. E. G.-B.

Notes and references

1 C. T. Kresge, M. E. Leonowicz, W. J. Roth, J. C. Vartuli and J. S. Beck, *Nature*, 1992, **359**, 710.
2 Q. Huo, R. Leon, P. M. Petroff and G. D. Stucky, *Science*, 1995, **268**, 1334.
3 Q. Huo, D. I. Margolese and G. D. Stucky, *Chem. Mater.*, 1996, **8**, 1147.
4 J. M. Thomas, *Nature*, 1994, **368**, 289.
5 J. M. Thomas, *Angew. Chem., Int. Ed.*, 1999, **38**, 3589.
6 Y.-J. Han, G. D. Stucky and A. Butler, *J. Am. Chem. Soc.*, 1999, **121**, 9897.
7 H. H. P. Yiu, C. H. Botting, N. P. Botting and P. A. Wright, *Phys. Chem. Chem. Phys.*, 2001, **3**, 2983.
8 D. Zhao, Q. Huo, J. Feng, B. F. Schmelka and G. D. Stucky, *J. Am. Chem. Soc.*, 1998, **120**, 6024.
9 V. Alfredsson and M. W. Anderson, *Chem. Mater.*, 1996, **8**, 1141.
10 S. Che, Y. Sakamoto, O. Terasaki and T. Tatsumi, *Chem. Mater.*, 2001, **13**, 2237.
11 Y. Sakamoto, M. Kaneda, O. Terasaki, D. Y. Zhao, J. M. Kim, G. D. Stucky, H. J. Shin and R. Ryoo, *Nature*, 2000, **408**, 449.
12 W. Zhou, H. M. A. Hunter, P. A. Wright, Q. Ge and J. M. Thomas, *J. Phys. Chem. B*, 1998, **102**, 6934.
13 J. M. Thomas, O. Teresaki, P. L. Gai, W. Zhou and J. Gonzalez-Calbet, *Acc. Chem. Res.*, 2001, **34**, 583.
14 C. E. Fowler, D. Khushalani and S. Mann, *J. Mater. Chem.*, 2001, **11**, 1968.

15 H. Yang, G. Vovk, N. Coombs, I. Sokolov and G. A. Ozin, *J. Mater. Chem.*, 1998, **8**, 743.
16 M. Stocker, *Microporous Mesoporous Mater.*, 2000, **38**, 1.
17 H. M. A. Hunter and P. A. Wright, *Microporous Mesoporous Mater.*, 2001, **43**, 361.
18 R. Zana, M. Benrraou and R. Rueft, *Langmuir*, 1991, **7**, 1072.
19 S. Schacht, Q. Huo, I. G. Voigt-Martin, G. D. Stucky and F. Schüth, *Science*, 1996, **273**, 768.
20 M. Grun, I. Lauer and K. K. Unger, *Adv. Mater.*, 1997, **9**, 254.
21 I. Diaz, F. Mohino, E. Sastre and J. Perez-Pariente, *Zeolites and Mesoporous Materials at the Dawn of the 21st Century, Proc. 13th IZC*, ed. A. Galarneau, F. di Renzo, F. Fajula and J. Vedrine, *Stud. Surf. Sci. Catal.*, 2001, **135**, 285.